State Planning and Research Program
Quarterly Report

PROJECT TITLE: Design and Construction Guidelines for Thermally Insulated Concrete Pavements

OBJECTIVES:
The main objective of the proposed research is to develop design and construction guidelines for thermally insulated concrete pavements (TICP), i.e. composite thin HMA overlays of new or structurally sound existing PCC pavements. A secondary objective is to develop recommendations for feasibility analysis of newly constructed TICP or thin overlays of the existing concrete pavements.

PERIOD COVERED: October 1 – December 31, 2009

PARTICIPATING AGENCIES: Minnesota Department Of Transportation, Caltrans, Federal Highway Administration, Local Road Research Board, Washington State Department of Transportation

PROJECT MANAGER: Tim Clyne **LEAD AGENCY**: Minnesota Dept. of Transportation **PRINCIPAL INVESTIGATOR**: Lev Khazanovich	**SP&R PROJECT NO**: TPF 5(149)	PROJECT IS: _____ Planning __X__ Research & Development
ANNUAL BUDGET: The total project budget is $455,000. Of that $16,000 is reserved for pooled fund administrative costs, which leaves $439,000 available for research.	**PROJECT EXPENDITURES TO DATE**: The estimated expenses are $140,400.	

WORK COMPLETED:
See attached.

SUMMARY OF ACTIVITIES EXPECTED TO BE PERFORMED NEXT QUARTER:
The research team will finalize validation of the MEPDG EICM model and will continue work on improvements to the MEPDG structural models.

STATUS AND COMPLETION DATE:
All work is on schedule.

Task 3. EICM Validation and Analysis

Temperature data from cells 106 and 206 at MnROAD were processed in order to determine the quality of the data. The data was processed using statistical analysis tools developed by Dr. Randal J. Barnes at the University of Minnesota.

Background

Cell 106 and Cell 206 are AC over PCC composite pavements located on the mainline section at the MnROAD test facility. Sensors were installed at various depths throughout the pavement.

Analysis

Previously, temperature data was analyzed from MnROAD test sections 106 & 206. The temperature data was screened, and data that was suspected to be erroneous was flagged. A table indicating the percentage of un-flagged data from each sensor in cell 106 & 206 was presented.

The following analysis was performed for Cell 106. The difference in temperature was determined for four similar sensor pairings; the temperature of the uppermost sensor located in the PCC layer of the pavement structure minus the temperature of the bottom sensor in the PCC layer. The four sensor pairings that were analyzed in Cell 106 were: 104 & 106, 112 &114, 120& 122, and 128 & 130. These sensors were selected because they were the sensors located closest to the top and bottom of the PCC layer. The pairings were selected because the sensors are similar in that they are located at the same depth, and in the exact same pavement structure, but at varying locations.

Cell	Model	Sensor	Depth (ft)	Depth (in)
106	TC	104	0.208	2.496
106	TC	106	0.5	6
106	TC	112	0.208	2.496
106	TC	114	0.5	6
106	TC	120	0.208	2.496
106	TC	122	0.5	6
106	TC	128	0.208	2.496
106	TC	130	0.5	6

The depth listed in the table is from the top surface of the pavement. Cell 106 is a composite pavement structure, with a 2-in AC layer on top of a 5-in PCC layer. It is noted that the "top" sensors were located approximately ½ - in below the top surface of the PCC layer, and the "bottom" sensors were located 1-in above the bottom surface of the PCC layer.

The difference in temperature between the top and bottom sensors were determined for each sensor pairing, and plotted on the following histograms.

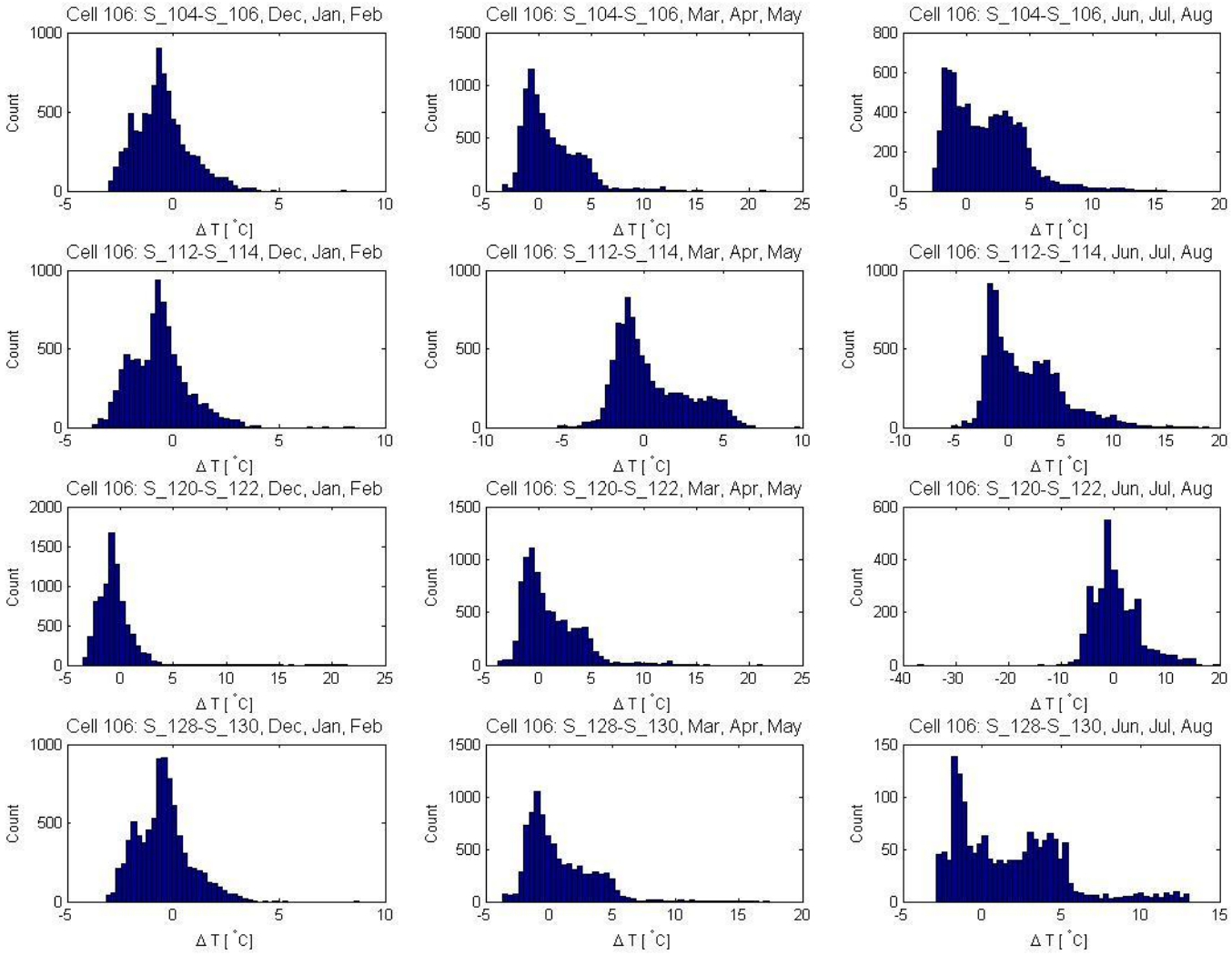

The delta-T "bins", located on the X-axis, indicate the difference in temperature from the top and bottom sensors. The "Count" or frequency, located on the Y-axis, represents the number of observations that occurred in each particular bin. The data covered a 9-month time span: December 2008 – August 2009. The histograms are organized in rows according to sensor pairing (e.g. sensors 104-106 are located in the top row), and in columns according to season (e.g. each sensor pairing represents data from the months of Dec, Jan, and Feb in the leftmost column).

Given the organization of the histograms, it is expected that the histograms should look somewhat similar within each column, since the columns are representations of

temperature differences from the same season, as observed by different sensor pairings. It is noted that the differences in temperature from the top to the bottom of the PCC layer are more pronounced in the summer months, when the pavement structure is subjected to longer and more intense periods of incoming solar radiation. During periods where the incoming radiation is less intense (Dec, Jan, Feb) the differences in temperature are not as large.

Additionally, temperature data from Cells 106, 206, 113, 213, and 313 are currently undergoing screening and analysis.

Task 4. Evaluation of Pavement Response Models

This section reports the following:

- Comparison of ABAQUS vs. ISLAB with regards to wheel load only,
- Comparison of ABAQUS vs. ISLAB with regards to temperature load only, and
- Modification of Benedetto et al. model for creep compliance.

1. Comparison of Wheel Load Only Case between ABAQUS and ISLAB

The objective of this task is to establish similarity of solutions (stress and strain) between ABAQUS and ISLAB for elastic materials using a single wheel load. ISLAB has advantage over ABAQUS in terms of computational efficiency as the run-time is usually low. However, the analysis in ISLAB is valid only for elastic materials. Therefore, if the similarity of the solution is proven between ISLAB and ABAQUS for elastic materials, the analysis can be extended to other material models including viscoelastic and elasto-plastic using ABAQUS.

The structure includes an elastic PCC layer resting on subgrade with Winkler foundation. Firstly, a slab with the properties given in Table 1 was designed and analyzed in ISLAB 2005. [1]

Table 1. Input properties of the designed pavement slab in ISLAB.

Type	**Property**	**Value**
Structure	Length	180 in
	Width	144 in
Mesh	Elements (Length)	30
	Elements (Width)	24
Layer 1 – PCC	Element type	Plate
	Thickness	5 in

[1] *It should be noted that ISLAB uses a different X-Y coordinate system where X-axis denotes the Cartesian Y-axis and vice versa. This section of the report is written in terms of Cartesian X-Y coordinate system and should be appropriately modified for use into ISLAB.*

	Elastic Modulus	4e6 psi
	Poison's Ratio	0.25
Subgrade	K (Winkler)	100 psi/in
Load	Single Wheel (b/a)	1
	Tire pressure	100 psi
	Footprint	12 in x 12 in
	Load	14400 lb
	Location (start)	84.0 , 0.0

Figure 1 shows the graphic user interface (GUI) for the inputs to ISLAB 2005. It also displays the mesh and the location and size of the load. ISLAB utilizes 4-node plate elements with 3 degrees of freedom (D.O.F.) to analyze the structure in pure bending when no crack is present. It processes 5 D.O.F. when a crack is present due to horizontal movements along with the bending caused by jump in the neutral axis. The analysis was run and the output was recorded.

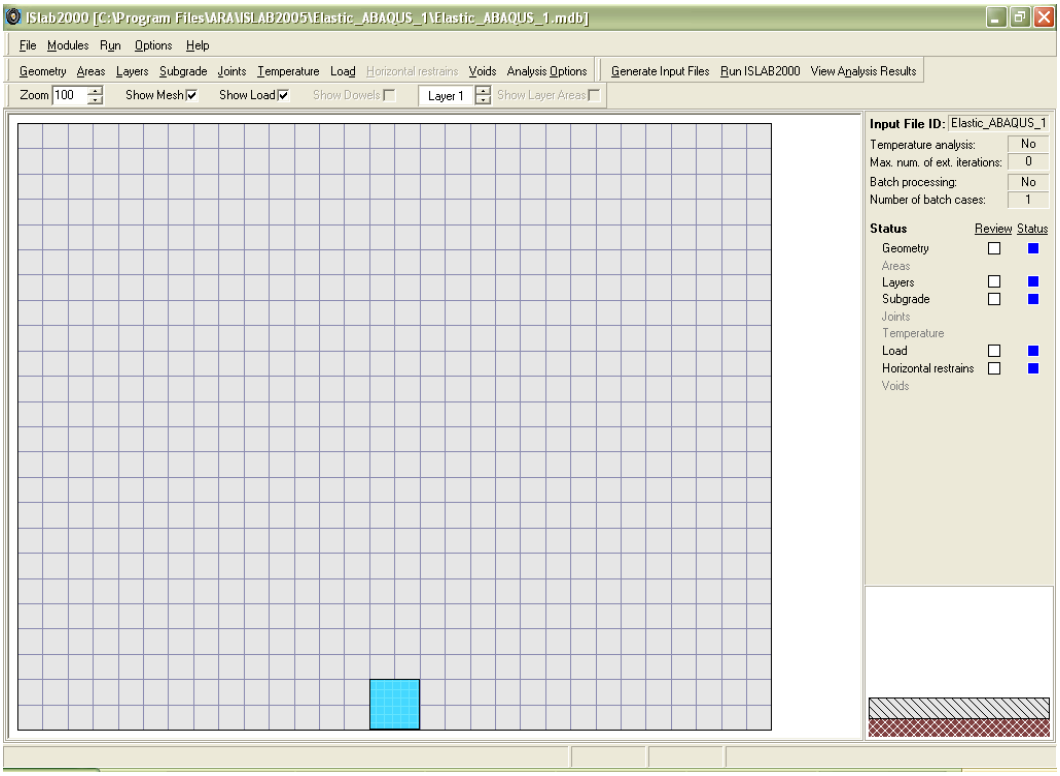

Figure 1. Input screen for ISLAB – single wheel loading.

For the ABAQUS analysis, a 3D model was designed which includes an elastic PCC layer resting on subgrade with Winkler foundation. The design properties of the slab are given in Table 2.

Table 2. Input properties of the designed pavement slab in ABAQUS.

Type	**Property**	**Value**
Structure	Length	180 in
	Width	144 in
	Thickness	5 in
Mesh	Element type	C3D8R / C3D20R

Layer 1 – PCC	Elastic Modulus	4e6 psi
	Poison's Ratio	0.25
Subgrade	K (Winkler)	100 psi/in
Load	Single Wheel (b/a)	1
	Tire pressure	100 psi
	Footprint	12 in x 12 in
	Location (start)	84.0, 0.0, 5.0

The slab was modeled with two different types of elements namely, continuum 3D 8-node reduced integration (C3D8R) brick elements and continuum 3D 20-node reduced integration (C3D20R) brick elements. Figure 2 presents the slab with C3D8R elements. Since each element has 8 nodes and 1 reduced integration point, a large number of elements are required to represent the slab. This increases the computational time of the analysis. Therefore, the mesh was adapted according to the accuracy of the intended solution. More elements were assigned closer to the wheel load than the other regions of the slab. To ensure computational accuracy an element size of 0.5 in was maintained across the thickness of the slab.

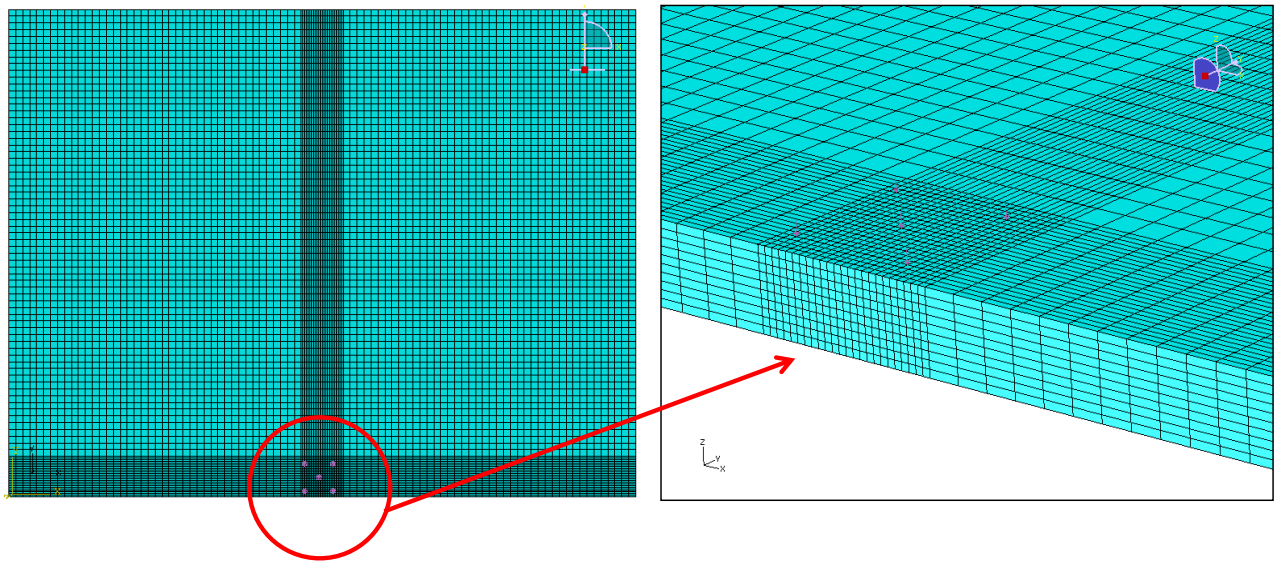

Figure 2. Slab model in ABAQUS with 8-node reduced integration brick element (C3D8R).

On the other hand, C3D20R elements were assigned to the slab as shown in figure 3. Since each element has 20 nodes and resulting 4 reduced integration points, the computational accuracy and efficiency are much greater than the C3D8R elements. In order to ensure computational accuracy an element size of 0.5 in was maintained across the thickness of the slab, as with C3D8R elements.

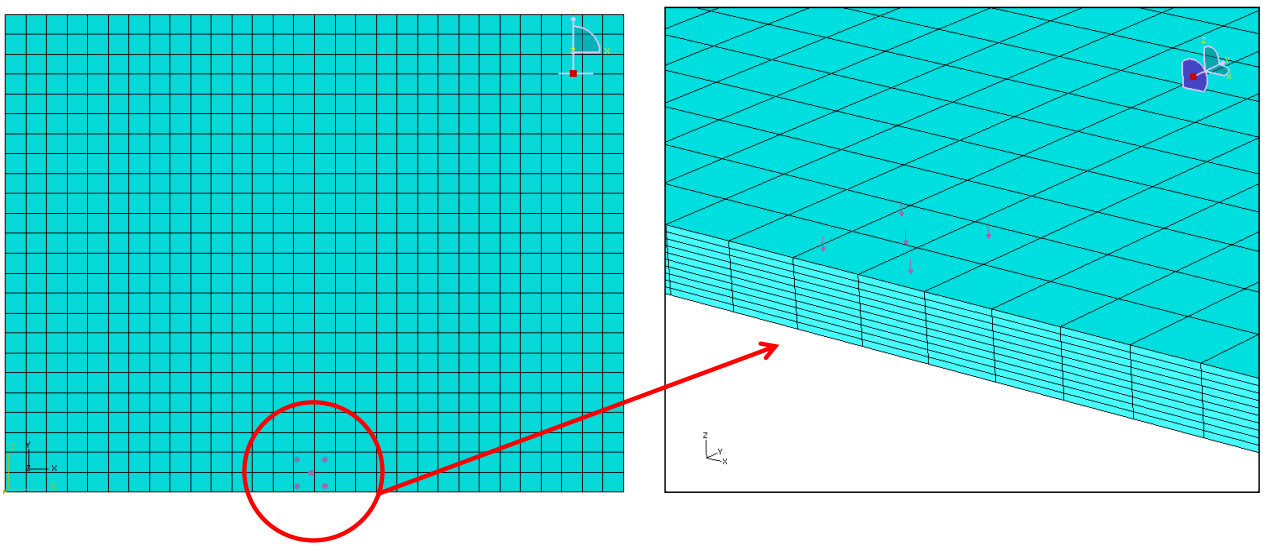

Figure 3. Slab model in ABAQUS with 20-node reduced integration brick element (C3D20R).

The deflection profile of the slab and the stresses at the bottom of the PCC layer were used to match the results from the ISLAB analysis to the ABAQUS analysis. The slab deflections (maximum and minimum) and the PCC stresses are tabulated in Table 3 for the various cases executed.

Table 3. Results from ISLAB and ABAQUS runs.

	ISLAB							
	Case	Mtr	Mesh	Load	S-Y dir	Max Uz	Min Uz	
	Elastic_ABAQUS_1	Elastic	30 x 24	100 psi	1248	0.0809	0.0079	
ABAQUS								
CAE	Job	Mtr	Mesh	Load	S11	Max Uz	Min Uz	ABAQUS:ISLAB
Elastic_ISLAB_1	Elastic_ISLAB_1	Elastic	C3D8R 720 (D)	100 psi				
Elastic_ISLAB_2	Elastic_ISLAB_2	Elastic	C3D8R 720	100 psi				
	Elastic_ISLAB_3	Elastic	C3D8R 32400	100 psi	937.4			75.11
	Elastic_ISLAB_4	Elastic	C3D8R 74880	100 psi	1044	0.08290	0.0078	83.65
	Elastic_ISLAB_5	Elastic	C3D8R 37440	100 psi	948.8	0.08400	0.0078	76.03
	Elastic_ISLAB_6	Elastic	C3D8R 97200	100 psi	1050	0.08280	0.0078	84.13
Elastic_ISLAB_3	Elastic_ISLAB_7	Elastic	C3D20R 3600	100 psi	1232	0.08276	0.0078	98.72
	Elastic_ISLAB_8	Elastic	C3D20R 7200	100 psi	1235	0.08276	0.0078	98.96

As stated before, ISLAB employs 4-node plate elements with 3 D.O.F. to analyze the structure. For the ABAQUS cases, the C3D8R elements matched up to 84% of the PCC stress obtained from ISLAB. Increasing the number of elements from ~75K to 97K resulted in an increase of only 6 psi (< 1%). It also predicted higher deflections than ISLAB analysis.

The use of C3D20R elements matched the ISLAB results very well (PCC stress ~ 99%). Also, the computation time was less than 1 minute. However, it must be noted that there is difference in the predicted displacement of the slab between the ISLAB and ABAQUS

analyses. Figures 4 and 5 display the deflection profile of the slab for the ISLAB and ABAQUS analyses, respectively.

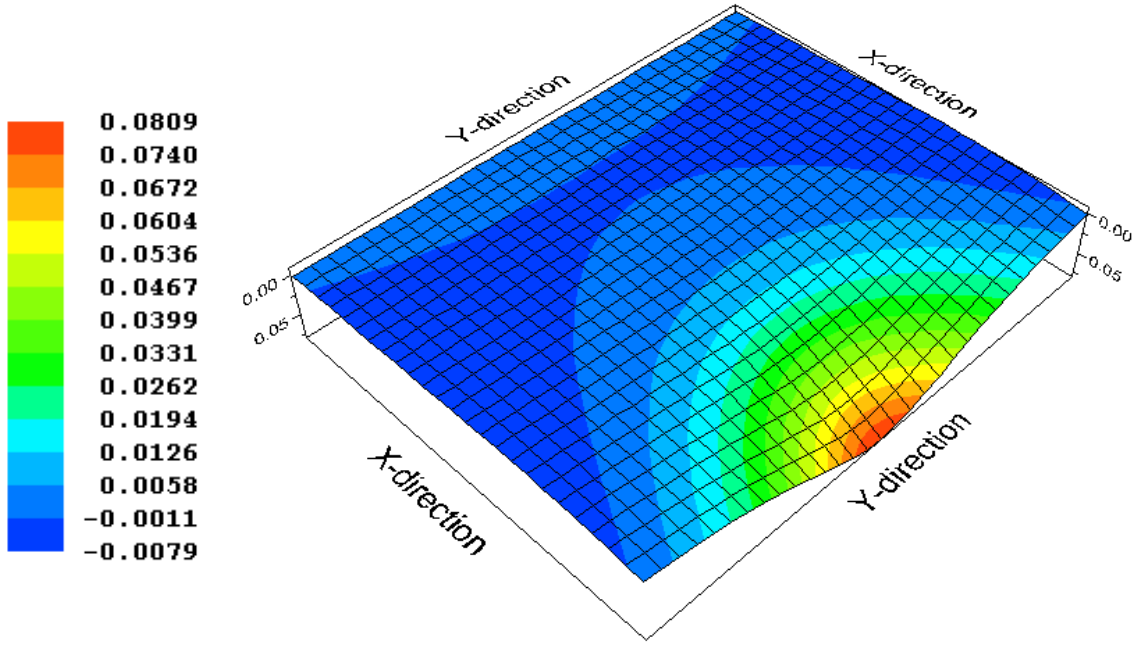

Figure 4. Deflection profile of the slab – ISLAB.

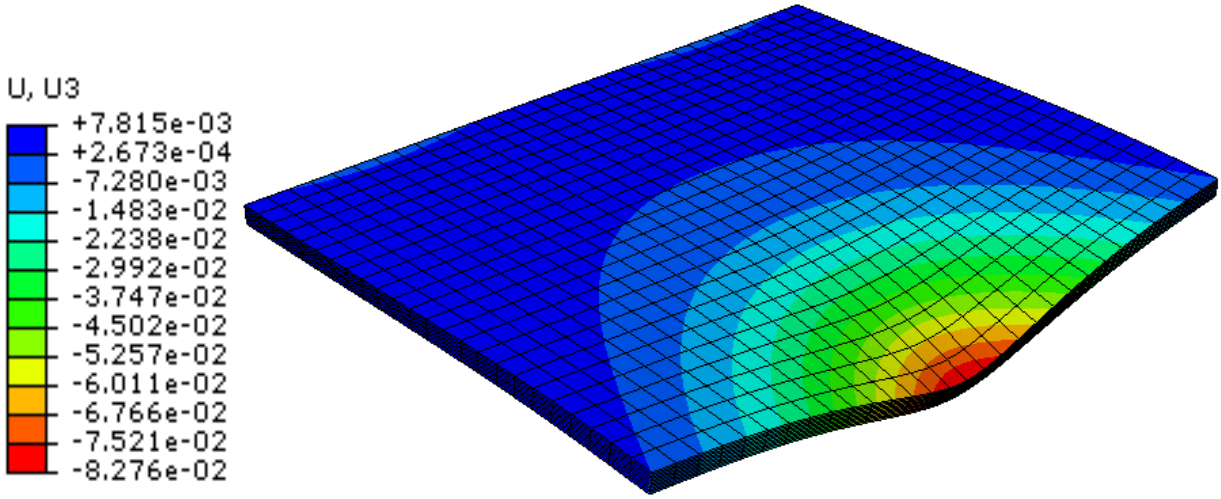

Figure 5. Deflection profile of the slab with C3D20R elements – ABAQUS.

Figures 6 and 7 show the stress at the bottom of the PCC layer for the ISLAB and ABAQUS analyses, respectively.

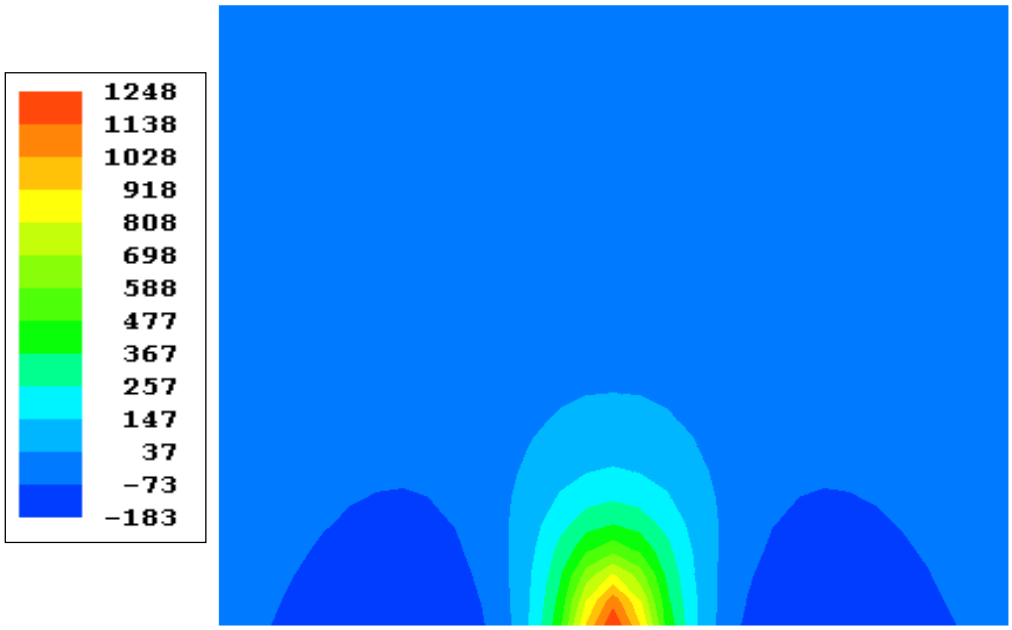

Figure 6. Stresses under the PCC layer in the direction of traffic – ISLAB.

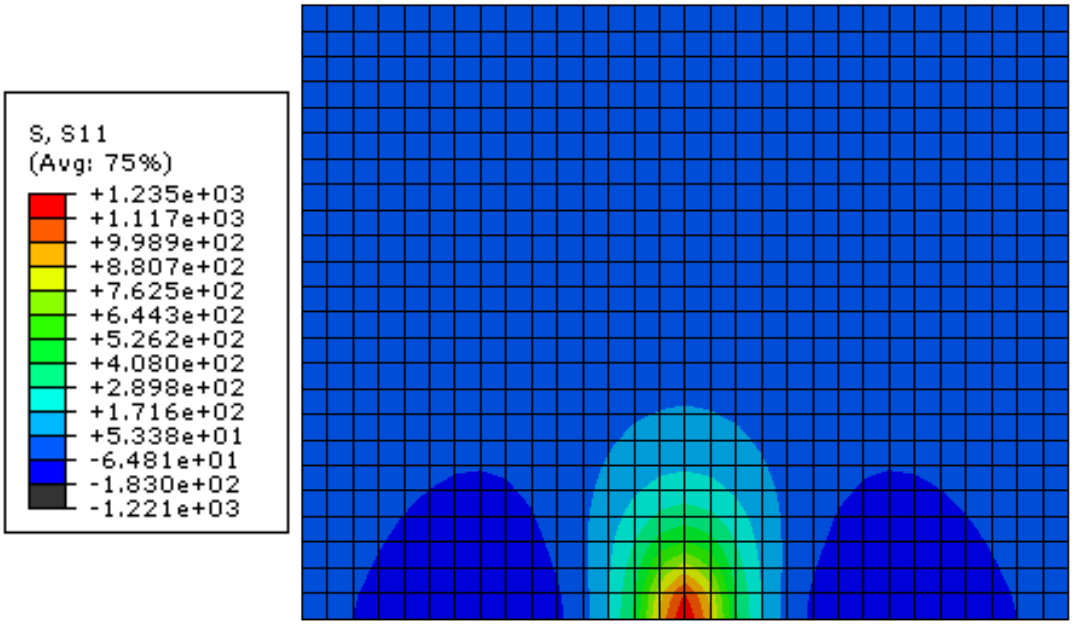

Figure 7. Stresses under the PCC layer in the direction of traffic with C3D20R elements – ABAQUS.

For the 'wheel load only' case, C3D20R elements in ABAQUS match the results from the ISLAB results closely. However, these needs to be verified for the 'temperature analysis only' case as well. The next section discusses the results from ISLAB and ABAQUS for the 'temperature analysis only' case.

2. Comparison of Temperature Only Case between ABAQUS and ISLAB

The objective of this task is to establish similarity of solutions (stress and strain) between ABAQUS and ISLAB for temperature loading. A secondary purpose is also to establish how subgrade stiffness (K-value) is deciphered in both the programs.

As there is no wheel load on the system it is important to consider the self-weight of the PCC slab. The structural and material input properties of the slab are given in Table 1 above. The slab was subjected to a linear temperature gradient with a difference of 30° between the top and bottom surface. The Winkler foundation option in ISLAB was selected to model the subgrade support. The curling of the slab due to the daytime temperature gradient causes a void under the center of slab as a result of separation from the foundation. The night-time temperature gradient causes a void under the edges of the slab. Figure 8 shows the graphic user interface (GUI) for the inputs to ISLAB 2005.

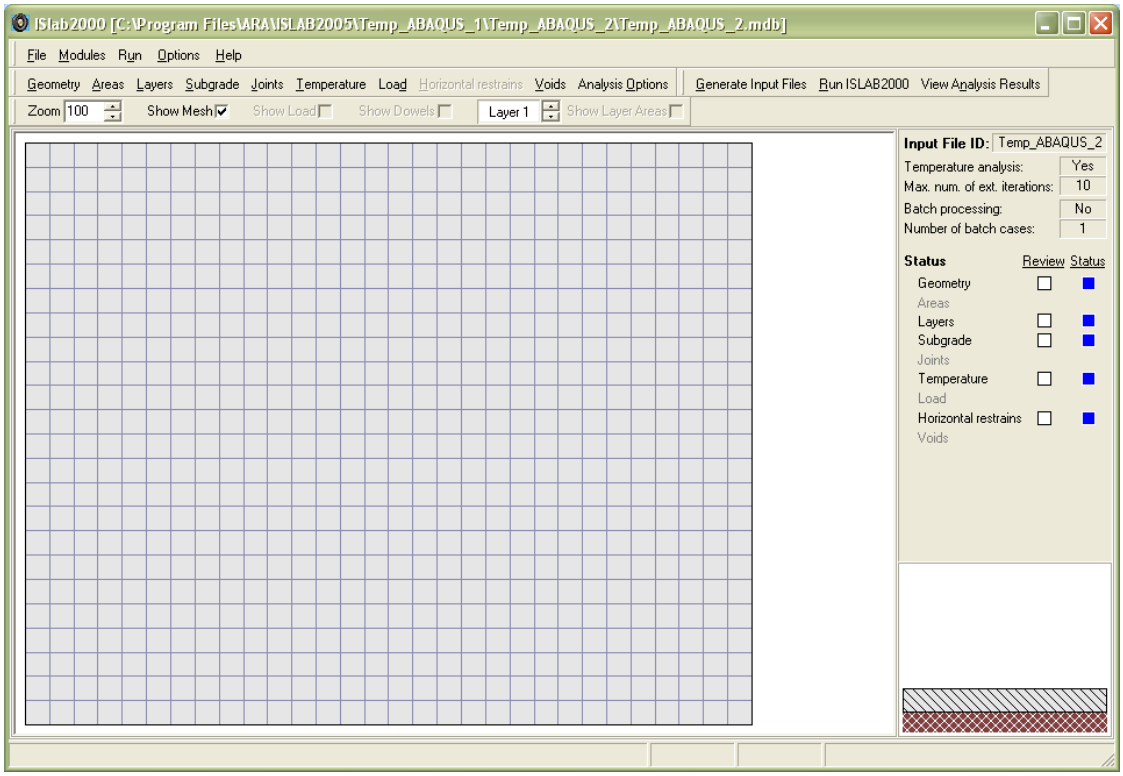

Figure 8. Slab loaded only under temperature loads in ISLAB.

Similarly, a slab was modeled in ABAQUS using the same structural and material properties as discussed above. The slab was also loaded with a linear temperature gradient of 30° between the top and bottom surface. The mesh, as generated on the slab, is shown in Figure 9.

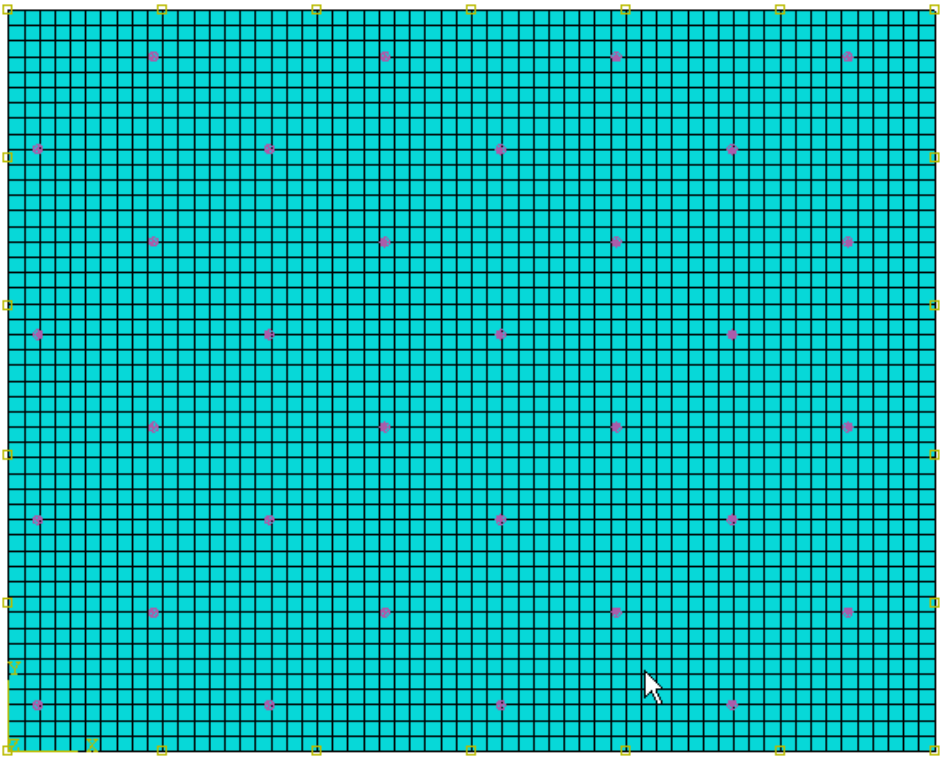

Figure 9. Slab loaded under temperature loads only in ABAQUS with mesh.

The subgrade support in ABAQUS is modeled using elastic foundation. The foundation pressure acts normal to the face of the element and rotates with the element face during large deformations. As a result, the foundation never detaches from the base of the slab. The difference between ISLAB and ABAQUS foundation model is apparent when the self-weight of the slab is low. However, if the self-weight is increased, the difference between the deformations was found to be insignificant. Table 4 tabulates the results from the comparative analysis for different self-weights and mesh sizes in ABAQUS.

Table 4. Results from ISLAB and ABAQUS runs from temperature only analysis.

	ISLAB										γh/k
h	Case	γ	p	Mtr	Mesh	Δ Temp	S-Y dir	Max Uz	Min Uz	max - min	self wt
5	Temp_ABAQUS_1	0.087	0.435	Elastic	30 x 24	30	281	0.0629	-0.056	0.1189	0.00435
	Temp_ABAQUS_6	0.314	1.57	Elastic	30 x 24	30	432	0.0647	0	0.0647	0.01570
	Temp_ABAQUS_2	10	50	Elastic	30 x 24	30	432	0.549	0.4843	0.0647	0.50000
	ABAQUS										
CAE	Job	γ	**p**	Mtr	Mesh	Δ Temp	S11	Max Uz	Min Uz	max - min	self wt
Temp_ISLAB_1	Temp_ISLAB_1	0.087	0.435	Elastic	3600	30	347	0.0524	-0.0131	0.0655	0.00435
	Temp_ISLAB_3	0.314	1.57	Elastic	3600	30	347	0.0638	-0.0018	0.0656	0.01570
	Temp_ISLAB_4	10	50	Elastic	3600	30	347	0.5480	0.4826	0.0654	0.50000
	Temp_ISLAB_5	10	50	Elastic	14400	30	346.9	0.5480	0.4826	0.0654	0.50000
Temp_ISLAB_2	Temp_ISLAB_6	10	50	Elastic	28800	30	388	0.5486	0.4822	0.0664	0.50000
Temp_ISLAB_3	Temp_ISLAB_7	10	50	Elastic	C3D20R 7200	Does not work because of 2 integration points					

Figures 10 and 11 display the deflection profile of the slab for the ISLAB and ABAQUS

analyses for a temperature gradient of 30° between the top and the bottom of the slab, respectively.

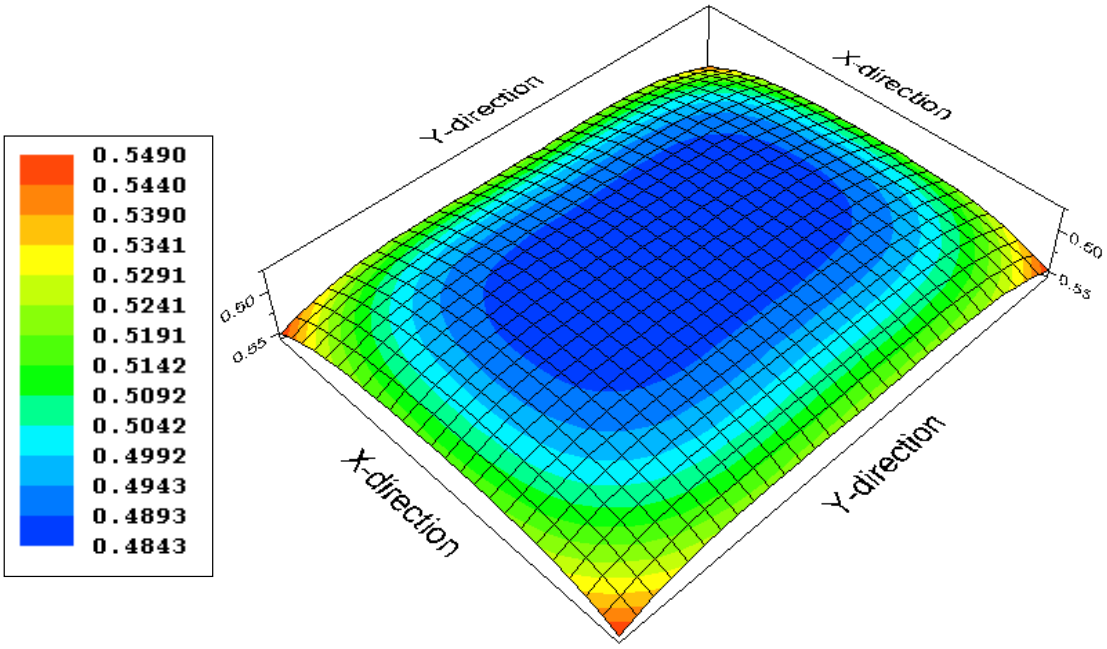

Figure 10. Deflection profile of the slab under large self-weight for the ISLAB temperature only analysis.

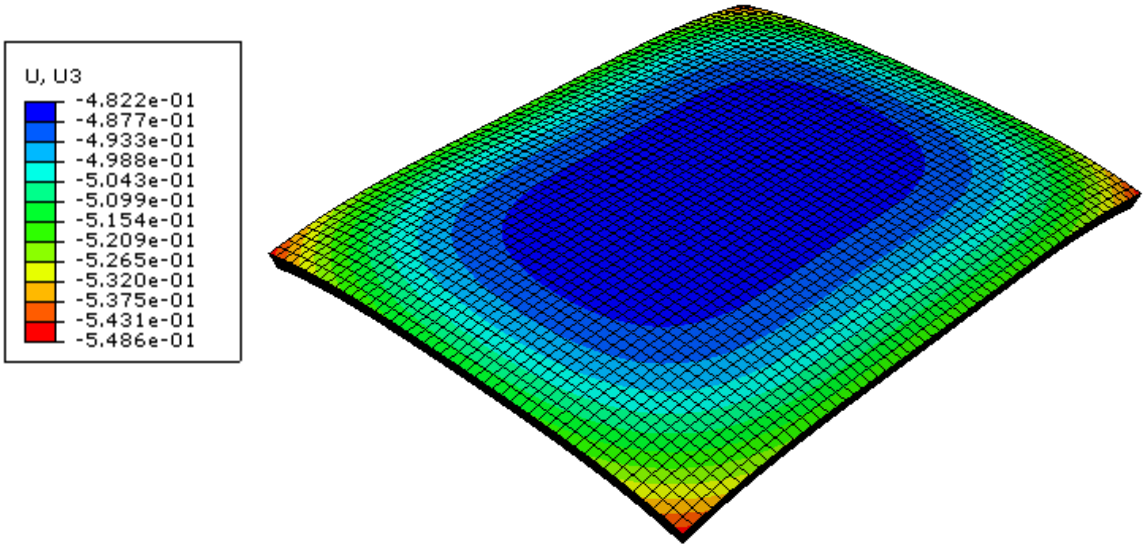

Figure 11. Deflection profile of the slab under large self-weight for the ABAQUS temperature only analysis.

The deflection profiles are found to be similar. It should be noted that the ABAQUS results are using the C3D8R and not C3D20R mesh elements. Figures 12 and 13 show the stress at the bottom of the PCC layer for the ISLAB and ABAQUS analyses, respectively.

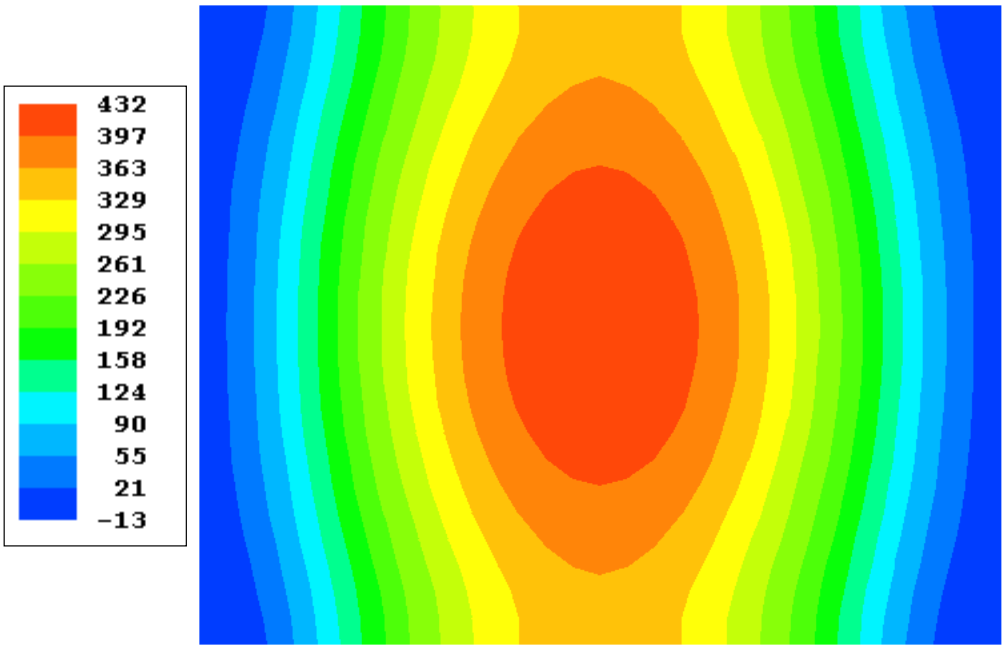

Figure 12. Stress under the PCC layer in the direction of traffic – ISLAB.

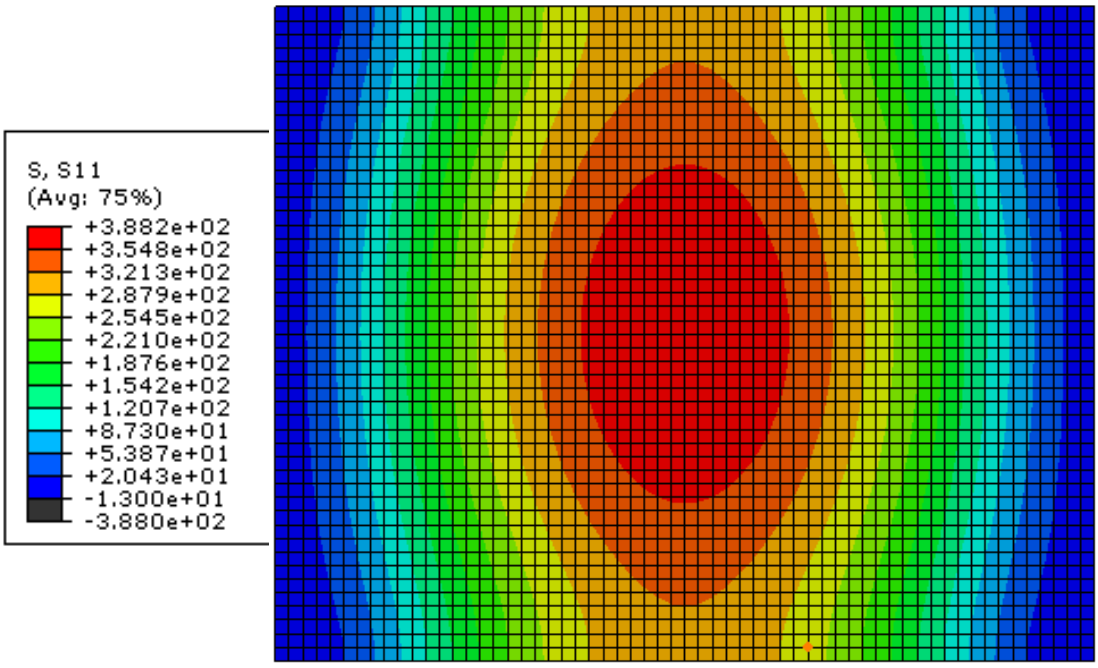

Figure 13. Stress under the PCC layer in the direction of traffic with C3D8R elements – ABAQUS.

The stress profiles as well as the magnitudes are similar between the ISLAB and the ABAQUS analyses. However, it should be noted that this analysis could not be performed in ABAQUS using the C3D20R elements. Figures 14 and 15 demonstrate the C3D8R and C3D20R elements, respectively.

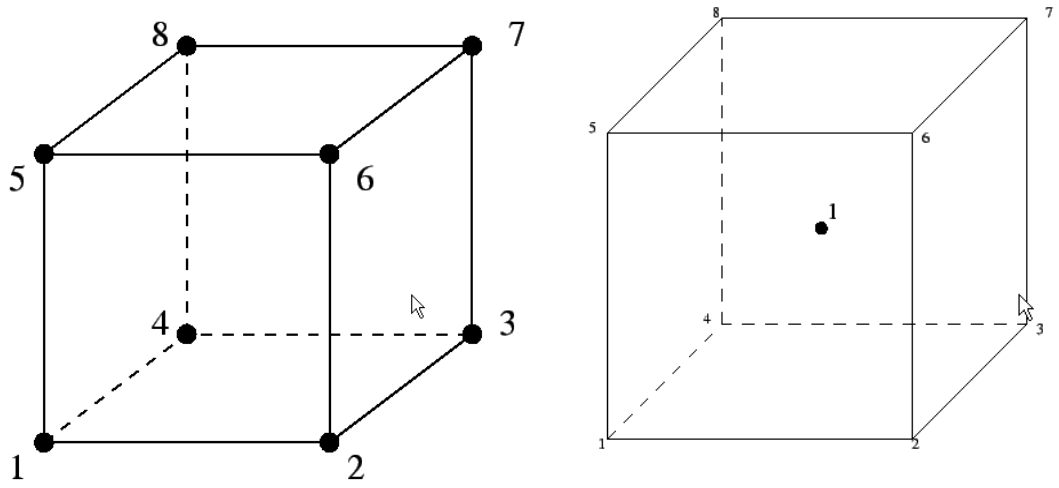

Figure 14. The 3 dimensional 8-node continuum element with 1 reduced integration point.

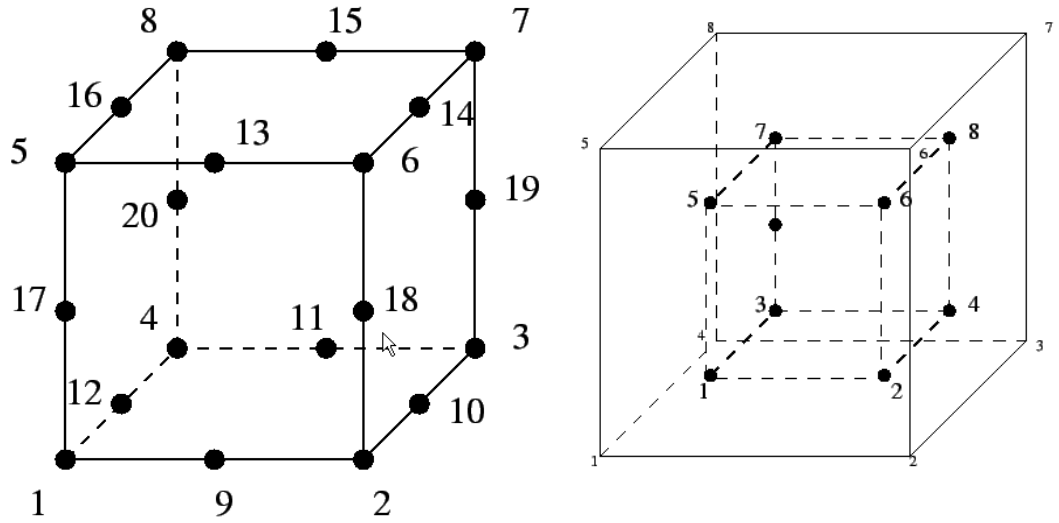

Figure 15. The 3 dimensional 20-node continuum element with 8 reduced integration point.

This is so because when a temperature gradient is assigned to a C3D8R element, the average temperature is assigned to the reduced integration point which is at the center of the element. Therefore, a C3D8R element has a uniform temperature gradient. However, in case of C3D20R elements due to the presence of 2 planes of integration points (1-2-3-4 and 5-6-7-8), the weighted average temperature is assigned at each plane. As no temperature could be assigned to the center of the element, it is assumed to be equal to zero. As a result, an unintended uneven temperature field is applied to the element which is not representative of the original temperature gradient. Hence, C3D20R elements are not suitable to perform temperature analysis. This issue will be further investigated.

3. Modification of Benedetto et al. Analysis for Creep Compliance

A 15-element Benedetto et al. model for creep compliance $J(t)$ was considered given by eq. (1) and as shown in Figure 16. This material model can be used in ABAQUS to simulate the viscoelastic behavior of asphalt. However, in order to increase the computational efficiency of ABAQUS it may be useful to reduce the number of elements in the model while maintaining the viscoelastic behavior.

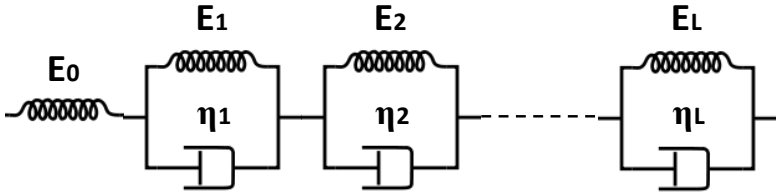

Figure 16. Benedetto et al's 15 element model for creep compliance.

$$J(t) = \frac{1}{E_0} + \sum_{l=1}^{L} \frac{1}{E_l}\left(1 - e^{\frac{-t}{\tau_l}}\right) \quad (1)$$

$$\tau = \frac{\eta}{E} \quad (2)$$

where: E_0 is the instantaneous spring stiffness,
E is the element spring stiffness,
η is the element viscosity,
L is the total number of elements in the model, and
t is the time in seconds.

Table 5 illustrates the values that were used to evaluate $J(t)$ using all 15 elements. All the elements in the Benedetto et al.'s model are assigned a factor of 1 or in other word are "on". Table 6 enlists the modified model with seven elements. In this case, the elements that are not considered in the model are assigned a factor of 0 and thus are "off". The stiffness of elements 8 to 15 was accounted in the initial spring stiffness E_0 by introducing the equivalent spring stiffness E_{eq} as follows:

$$\frac{1}{E_{eq}} = \frac{1}{E_0} + \frac{1}{E_8} + \frac{1}{E_9} + \frac{1}{E_{10}} + \frac{1}{E_{11}} + \frac{1}{E_{12}} + \frac{1}{E_{13}} + \frac{1}{E_{14}} + \frac{1}{E_{15}} \quad (3)$$

Table 5. Example values for Benedetto 15-element model.

Element Number	Spring Stiffness, El (psi)	Viscosity, ηl (psi.s)	τl	Factor
0	6380000	----		
1	95265	11307535	118.6956	1
2	101500	997600	9.828571	1
3	278110	332485	1.195516	1
4	789090	266075	0.337192	1
5	1014565	132965	0.131056	1
6	1300070	16675	0.012826	1
7	3562215	3335	0.000936	1
8	9769665	997.6	0.000102	1
9	12024270	298.7	2.48E-05	1
10	13151500	20.3	1.54E-06	1
11	28197715	1.595	5.66E-08	1
12	48097080	0.1595	3.32E-09	1
13	97697230	0.01595	1.63E-10	1
14	137527570	0.001653	1.2E-11	1
15	222448995	0.00009657	4.34E-13	1

Table 6. Example values for Benedetto 15-element model.

Element Number	Spring Stiffness, El (psi)	Viscosity, ηl (psi.s)	τl	Factor	Eeq	gi or ki
0	6380000	----			2013867	
1	95265	11307535	118.695586	1		0.01040615
2	101500	997600	9.828571429	1		0.011087223
3	278110	332485	1.195516163	1		0.03037899
4	789090	266075	0.337192209	1		0.086195237
5	1014565	132965	0.131056167	1		0.110824711
6	1300070	16675	0.012826232	1		0.142011485
7	3562215	3335	0.000936215	1		0.389114002
8	9769665	997.6	0.000102112	0		
9	12024270	298.7	2.48414E-05	0		
10	13151500	20.3	1.54355E-06	0		
11	28197715	1.595	5.65649E-08	0		
12	48097080	0.1595	3.31621E-09	0		
13	97697230	0.01595	1.63259E-10	0		
14	137527570	0.001653	1.20194E-11	0		
15	222448995	0.00009657	4.34122E-13	0		

Figures 17 and 18 compare the creep compliance $J(t)$ for the 15-element model and the modified 7-element model under short-term and long-term loading.

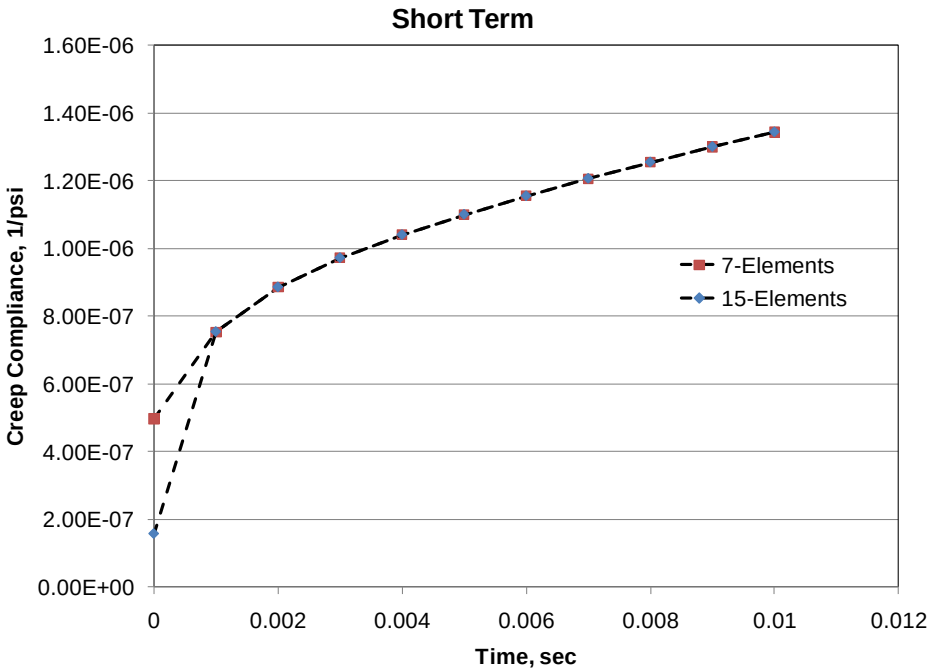

Figure 17. Short-term creep compliance versus time for 15-element and 7-element models.

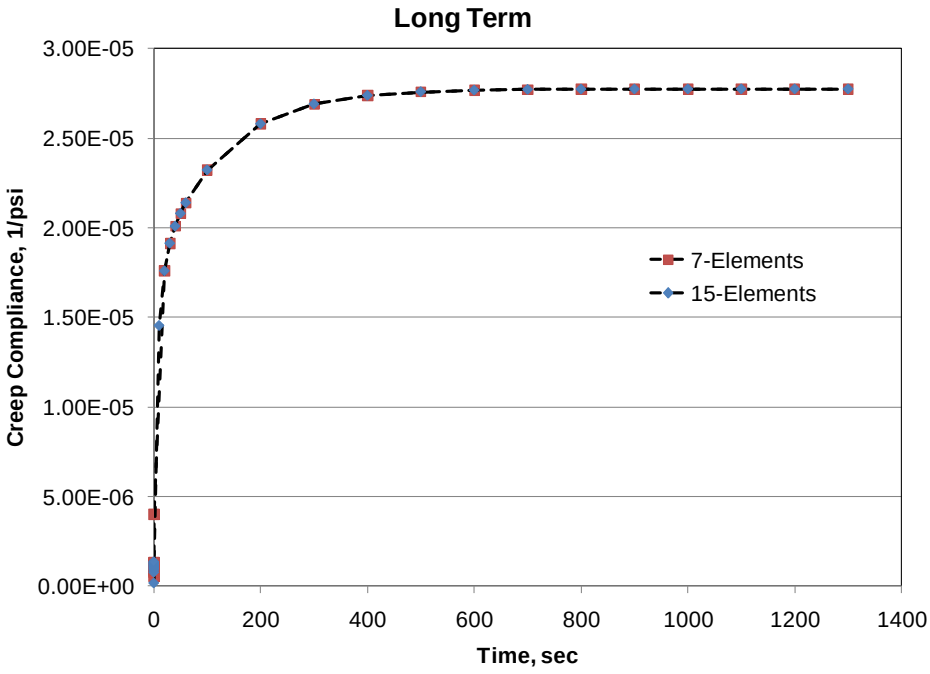

Figure 18. Long-term creep compliance versus time for 15-element and 7-element models.

Based on the above figures, it was concluded that the modified 7-element Benedetto et al.'s model is a valid representation of the viscoelastic behavior of a material that could be modeled in ABAQUS.